Electrocatalysis
https://doi.org/10.1007/s12678-019-00566-x

ORIGINAL RESEARCH

Enhanced Photoelectrocatalytical Performance of Inorganic-Inorganic Hybrid Consisting $BiVO_4$, V_2O_5, and Cobalt Hexacyanocobaltate as a Perspective Photoanode for Water Splitting

K. Trzciński[1] · M. Szkoda[1] · M. Sawczak[2] · A. Lisowska-Oleksiak[1]

Abstract

Thin layers of $BiVO_4/V_2O_5$ were prepared on FTO substrates using pulsed laser deposition technique. The method of cobalt hexacyanocobaltate (Cohcc) synthesis on the $BiVO_4/V_2O_5$ photoanodes consists of cobalt deposition followed by electrochemical oxidation of metallic Co in $K_3[Co(CN)_6]$ aqueous electrolyte. The modified electrodes were tested as photoanodes for water oxidation under simulated sunlight irradiation. Deposited films were characterized using UV-Vis spectroscopy, Raman spectroscopy, and scanning electron microscopy. Since the V_2O_5 is characterized by a narrower energy bandgap than $BiVO_4$, the presence of V_2O_5 shifts absorption edge (ΔE = ~0.25 eV) of modified films towards lower energies enabling the conversion of a wider range of solar radiation. The formation of heterojunction increases photocurrent of water oxidation measured at 1.2 V vs Ag/AgCl (3 M KCl) to over 1 mA cm^{-2}, while bare $BiVO_4$ and V_2O_5 exhibit 0.37 and 0.08 mA cm^{-2}, respectively. On the other hand, the modification of obtained layers with Cohcc shifts onset potential of photocurrent generation into a cathodic direction. As a result, the photocurrent enhancement at a wide range of applied potential was achieved.

Keywords Photoanode · Water splitting · Visible light activity · Pulsed laser deposition

Introduction

The scientific community has a moral obligation to take up efforts to reduce emissions of greenhouse gases. Photoelectrochemical water splitting is one of the most promising methods of hydrogen generation which is of great importance considering climate changes [1]. Sunlight energy conversion to environmentally desired fuel requires efficient photocatalysts. Since 1972, when Fujishima and Honda published their milestone paper [2], many different materials were tested as photoanodes for water photooxidation. Among them is bismuth vanadate, which exhibits high absorption coefficient [3] and a relatively narrow energy bandgap [4]. However, $BiVO_4$ suffers from poor kinetics of water oxidation and low mobility and separation efficiency of charge carriers [5]. There are many strategies of enhancement of the $BiVO_4$ photocatalytic properties that can minimize the main drawbacks [6]. One of them is based on the formation of heterojunction. It can be n-n [7] as well as n-p [8, 9] junction built from $BiVO_4$ and another semiconductor. The most commonly tested system is based on $BiVO_4$ and WO_3; however, $BiVO_4$ has been already combined with, e.g., $Bi_4V_2O_{11}$ [10], TiO_2 [11], and MnO_2 [12]. This manuscript is focused on the photoelectrochemical properties of $BiVO_4/V_2O_5$ bulk system. The photocatalytic and antibacterial properties of such a composite have been already studied, e.g., [13, 14]. Recently, $BiVO_4/V_2O_5$ junction has been characterized as a promising photoanode for water splitting. The various geometries of the junction (e.g., bulk, layer on layer) have been studied [15]. The V_2O_5 presence positively affects charge separation efficiency and light absorption ability due to the narrower energy bandgap. $BiVO_4$ was additionally doped using W atoms, and it leads to one of the highest photocurrents of water oxidation obtained for $BiVO_4$-based photoanodes [15]. Other authors claim that the presence of V_2O_5 in $BiVO_4/V_2O_5$ junction enhances mobility of charge carriers measured as transit time for the migration of photoexcited electrons to counter electrode, what was confirmed using intensity-

✉ K. Trzciński
trzcinskikonrad@gmail.com; kontrzci@pg.edu.pl

[1] Faculty of Chemistry, Gdańsk University of Technology, Narutowicza 11/12, 80-233, Gdańsk, Poland

[2] Centre for Plasma and Laser Engineering, The Szewalski Institute of Fluid Flow Machinery, Fiszera 14, 80-231 Gdańsk, Poland

Published online: 10 December 2019

modulated photocurrent spectroscopy [16]. The Bi/$BiVO_4$/V_2O_5 composite was obtained by annealing of pure bismuth vanadate powder in Ar/H_2 gas mixture. Obtained powder exhibited photocatalytic properties towards water oxidation reaction in $AgNO_3$ solution. The films of resulting material were tested as photoanodes, but only for hole scavenger photoelectrooxidation [17]. Significant enhancement of water oxidation photocurrent has been achieved for inverse opal heterostructure (V_2O_5/$BiVO_4$) modified using NiOOH due to the specific morphology, presence of the heterojunction, and electrode/electrolyte interface modified by cocatalyst [18].

The formation of a junction may positively affect the electron/hole pairs separation on the interface between the components as well as, in some cases, enhancing photoabsorption ability. Nevertheless, such a way of modification does not affect the surface recombination that takes place on the $BiVO_4$/electrolyte surface. The passivation of recombination centers and enhancement of oxygen evolution kinetics can be achieved *via* cocatalyst loading. $BiVO_4$-based photoanodes are commonly modified using oxygen evolution catalysts, i.e., FeOOH/NiOOH [19], cobalt phosphate (CoPi) [20], and cobalt borate [21]; however, the catalytic role of cocatalyst is not the most important. It is claimed that the presence of CoPi on $BiVO_4$ suppresses surface recombination and does not affect the kinetics of water oxidation [22]. However, appropriate cocatalyst on the top of $BiVO_4$ may affect both the kinetics of O_2 evolution reaction and inhibits surface recombination [23]. Thus, the discussion about the role of oxygen evolution cocatalysts in photoelectrochemical water splitting is still open.

Prussian blue analogues (PBA) are interesting group of oxygen evolution catalysts. Generally, the cobalt center coordinated by the nitrogen atoms from the cyanide group in PBA is essential to obtain efficient electrocatalyst [24]. However, the enhancement of photocurrent generation of water oxidation by $BiVO_4$ modified using nickel hexacyanoferrate has been also reported [25]. Some of PBA, e.g., cobalt hexacyanoferrate can accumulate photoexcited holes from $BiVO_4$, positively affecting the efficiency of photocurrent generation [26]. Thus, PBAs which exhibit electrocatalytic properties in oxygen evolution reaction can be successfully utilized to modification of electrode/electrolyte interface in $BiVO_4$-based photoanodes.

In the present work, bismuth vanadate was modified in two different ways. The first one is based on a formation of the $BiVO_4$/V_2O_5 bulk heterojunction. The phase of V_2O_5 can be formed from the excess of the V-source during the synthesis of $BiVO_4$. The thin films were prepared using pulsed laser deposition technique. The role of V_2O_5 in the photoelectrochemical water oxidation is discussed here. In order to enhance photocurrent generation in a wider range of applied potential, $BiVO_4$/V_2O_5 photoanodes were modified by cobalt hexacyanocobaltate (Cohcc) synthesize during two-step method. The choice of Cohcc is based on previous reports showing its catalytic activity towards water oxidation. Among tested cobalt hexacyanometalates, cobalt hexacyanocobaltate exhibited the lowest overpotential of water oxidation [24]. We have also reported previously that the presence of Cohcc on the $BiVO_4$ affects its photoelectrochemical performance as well [27]. Both ways of $BiVO_4$ modification enhance the efficiency of water splitting in a different way. In both cases, significant enhancement of anodic photocurrent has been demonstrated.

Experimental

Chemicals

FTO (fluorine-doped tin oxide) glass slides were purchased from Sigma and used as electrode substrates. Chemicals of analytical grade, $Bi(NO_3)_3{\cdot}5H_2O$, NH_4VO_3, V_2O_5, $K_3[Co(CN)]_6$ were supplied by Sigma-Aldrich. K_2SO_4, acetone, and isopropanol were supplied by POCH. The metallic Co target (TK 8900) for magnetron sputtering was purchased from Quorum. Triple distilled water was used for all electrochemical experiments.

Layer Preparation

The high-temperature solid-state chemical reaction using of $Bi(NO_3)_3{\cdot}5H_2O$ and an excess amount of NH_4VO_3 (the Bi:V molar ratio equals to 1:1.5) was used to obtain the $BiVO_4$/V_2O_5 powder *via* annealing at 500 °C for 5 h. The resulting mixture was homogenized and pressed into a pellet, and annealed again at 500 °C for 4 h. The $BiVO_4$/V_2O_5 pellet acted as a target for the pulsed laser deposition (PLD) technique. PLD was performed using a laser (Nd:YAG) equipped with a 4th harmonic generation module emitting 6 ns pulses at 266 nm (4 pulses per 1 s). The energy density of the laser was established at about 6.5 J cm^2. The deposition process was performed at room temperature in an oxygen atmosphere (p_{O2} ~1 10^{-2} mbar). Deposition took 60 min. Then, the samples were annealed in a tube furnace (PRC 55 L/1300 M, Czylok) for 2 h at 450 °C in air atmosphere (heating rate 2 °C/min) in order to obtain crystalline $BiVO_4$/V_2O_5 films. Deposition of FTO/V_2O_5 and FTO/$BiVO_4$ was performed for a comparison at the same conditions, but from separate targets, (a) V_2O_5 – pure oxide and (b) $BiVO_4$ (synthesized using equimolar amounts of $Bi(NO_3)_3{\cdot}5H_2O$ and NH_4VO_3).

The Cohcc deposition was performed according to the procedure reported in our previous report [27]. Briefly, it was a two-step method that consists (1) sputtering of a metallic cobalt using magnetron sputtering and (2) electrooxidation of Co film in 0.05 M $K_3[Co(CN)_6]$ + 0.1 M KCl electrolyte. As a result, FTO/$BiVO_4$/V_2O_5/Cohcc electrodes were obtained.

Research methods

The surface morphology was examined using scanning electron microscopy (SU3500, Hitachi). Raman spectra were recorded by a confocal micro-Raman spectrometer (InVia, Renishaw) with sample excitation, by means of an argon ion laser emitting at 514 nm and operating at 5% of its total power (50 mW). The transmittance of the samples was measured by UV-Vis spectrometer (Lambda 35, Perkin-Elmer). The spectra were registered in the range of 300–700 nm, with a scanning speed of 120 nm min^{-1}. The calibration of UV-Vis spectrometer was performed using bare FTO substrate.

The electrochemical and photoelectrochemical studies of materials were conducted using the AutoLabPGStat 302 N potentiostat-galvanostat system (Methrom, AutoLab) in the one-compartment three-electrode cell with a quartz window, where photoanode served as a working electrode (geometric surface area of ~0.5 cm^2). The Pt mesh with the high surface area was used as a counter electrode, while Ag/AgCl (3 M KCl) as a reference electrode. The electrochemical tests were carried out in deaerated 0.2 M K_2SO_4. Scan rate during photoelectrochemical measurements was equal to 20 mV s^{-1} A xenon lamp (LOT-QuantumDesign) equipped with AM 1.5 filter with a light intensity of 100 mW cm^{-2} was used as the light source.

Results and Discussion

Scanning Electron Microscopy

In order to investigate the surface morphology of annealed films, the SEM was employed. The SEM images of four films are presented in Fig.1. The film of V_2O_5 deposited using pulsed laser deposition technique crystallizes in the form of coarse, longitudinal crystals. Bismuth vanadate exhibits completely different morphology. The films are built from small grains with ~100–200 nm diameter. In the case of $BiVO_4/V_2O_5$ composite, the morphology is dominated by the presence of $BiVO_4$ grains. Elongated V_2O_5 crystals are not present in the SEM image. As can be observed, the grains forming the layer seem to be partially melted on the edges. It may be related to the presence of V_2O_5 that is characterized by the lower than $BiVO_4$ melting point (690 °C [28] and 940 °C [29], respectively). Films modified by cobalt hexacyanocobaltate are evenly covered by regular, cubic-shaped crystallites characteristic for metal hexacyanometallates [30]. The zoom of the ideal cube of Cohcc is shown in Fig. 1 inset.

Raman Spectroscopy

The Raman spectra of the V_2O_5, $BiVO_4$, $BiVO_4/V_2O_5$, and $BiVO_4/V_2O_5$/Cohcc are shown in Fig. 2. Samples showed characteristic bands of monoclinic structure $BiVO_4$ in 828, 709, 367, and 327 cm^{-1} [31]. A single band at 828 cm^{-1} is assigned to symmetric stretching V-O while the band at 709 cm^{-1} is attributed to the antisymmetric stretching V-O. The bands at 367 and 327 cm^{-1} are assigned to the symmetric and antisymmetric deformation V-O vibrations in VO_4^{3-} units, respectively. The bands at 213 and 130 cm^{-1} are attributed to external modes. The Raman spectrum of a film deposited from V_2O_5 target confirms that the sputtered layer consist only V_2O_5 [32]. In the case of the layer deposited from the $BiVO_4$ target with V-source excess, Raman spectrum of resulting layer consists of band characteristic for both bismuth vanadate and vanadium pentaoxide. No other phases are detected, confirming the formation of pure $BiVO_4/V_2O_5$ junction. Raman spectroscopy has been applied also in order to affirm the chemical structure of Cohcc. As it is shown in Fig. 2, the spectrum of $BiVO_4/V_2O_5$/Cohcc exhibits new bands in comparison of the film without Cohcc. The set of Raman bands at 2150–2230 cm^{-1} is characteristic for C ≡ N stretching vibration [33]. The presence of at least two bands at this region suggests that Co centers coexist at different oxidation states. The Raman band of Co-CN vibration at about 490 cm^{-1} are not clearly detected [34], probably due to the overlapping with bands coming from V_2O_5.

UV-Vis spectroscopy

The influence of V_2O_5 on the optical properties of tested films was investigated using UV-Vis spectroscopy in a transmittance mode, see fig. 3. The spectrum of bismuth vanadate film is characterized by an absorption edge typical for monoclinic $BiVO_4$ deposited onto transparent conductive oxide substrate [35]. The energy bandgaps were estimated from the absorption edges. The Tauc plot was not utilized here due to the difficulty to choose an appropriate type of an electron transition. $BiVO_4$ is characterized by allowed direct and allowed indirect transitions [3], while V_2O_5 by direct forbidden transition [32]. The one function cannot be used in order to determine a bandgap of $BiVO_4/V_2O_5$ heterojunction. The E_g of $BiVO_4$ was estimated to be equal to 2.45 eV. The edge seen on UV-Vis spectrum of V_2O_5 containing film is clearly shifted towards higher wavelengths. The lower energy bandgap of V_2O_5 enhances the absorption ability of the film in a visible range of electromagnetic radiation. The shift of absorption edge of about 0.25 eV is achieved due to the presence of V_2O_5 phase. It is not a very significant change; however, it should positively affect the photoactivity of investigated photoanodes. As it was reported, the absorbance of Prussian blue analogues is negligible due to the very low absorption

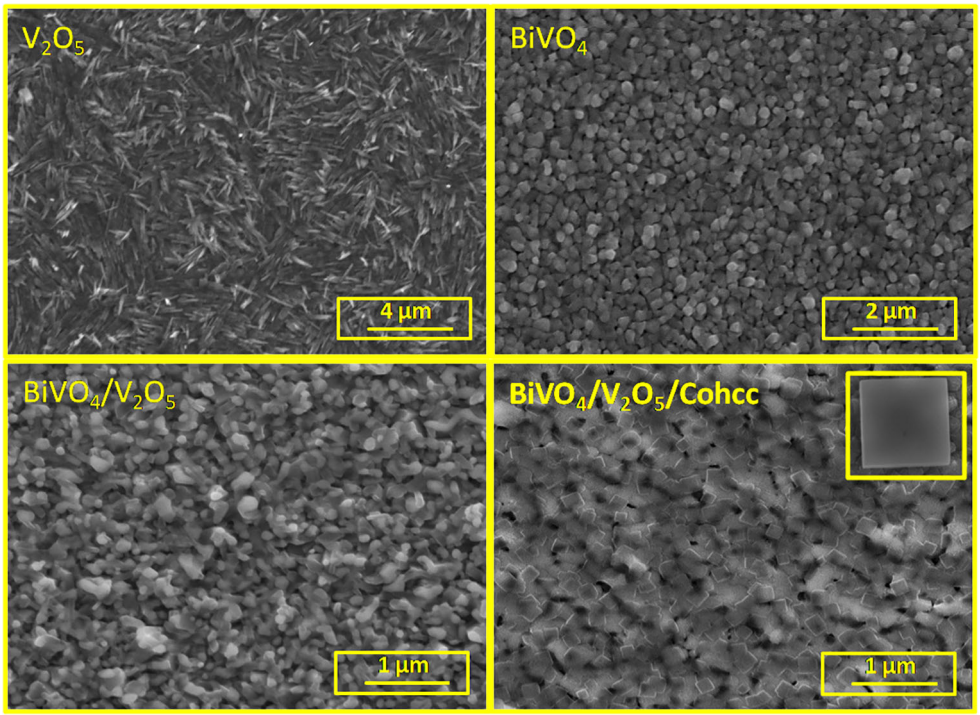

Fig. 1 SEM images of FTO/V_2O_5, FTO/$BiVO_4$/ FTO/$BiVO_4$/V_2O_5, and FTO/$BiVO_4$/V_2O_5/Cohcc

coefficient [36] in comparison with absorption coefficients of V_2O_5 and $BiVO_4$, and can be omitted in a discussion.

Photoelectrochemical Performance

In order to investigate the influence of the presence of V_2O_5 and Cohcc components on the photoelectrochemical properties of $BiVO_4$-based photoanodes, the linear sweep voltammograms were recorded under the illumination of the tested photoanodes. As it is shown in Fig. 4a, both $BiVO_4$ and V_2O_5 act as n-type semiconductors in contact with an aqueous electrolyte. Registered photocurrent measured at 1.2 V vs Ag/AgCl was equal to 90 and 370 µA cm^{-2} for V_2O_5 and $BiVO_4$, respectively. There is a significant difference of onset potential, where photocurrent is detectable. Photocurrent of water oxidation was generated at the much lower potential in the case of bismuth vanadate. Such an effect was expected due to the differences of flat-band potential of two photoanode materials [37]. The curve of V_2O_5 consists also a dark current anodic hump at 0.2–0.6 V. It was previously reported that at this range of applied potential, electrochemical oxidation with simultaneous Na^+ desorption occurs, what was confirmed using electrochemical quartz crystal microbalance and in situ Raman spectroscopy [38]. This phenomenon should be rather

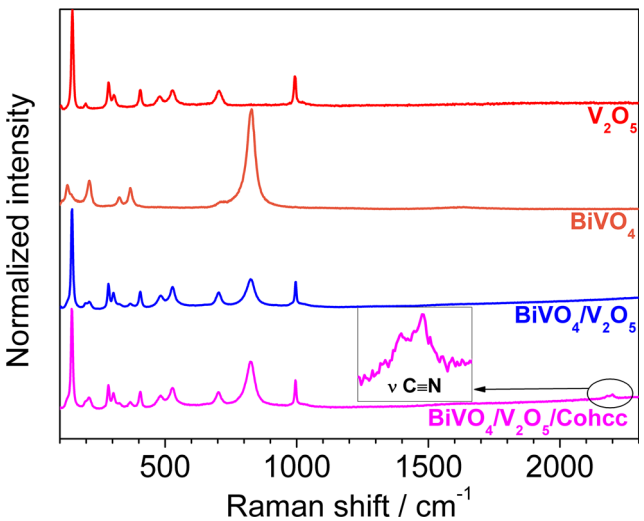

Fig. 2 Raman spectra of V_2O_5, $BiVO_4$, $BiVO_4/V_2O_5$, and $BiVO_4/V_2O_5$/Cohcc

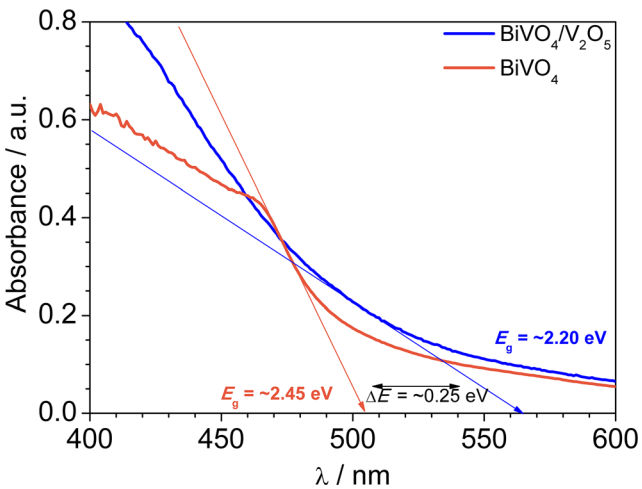

Fig. 3. UV-Vis spectra of $BiVO_4$ and $BiVO_4/V_2O_5$

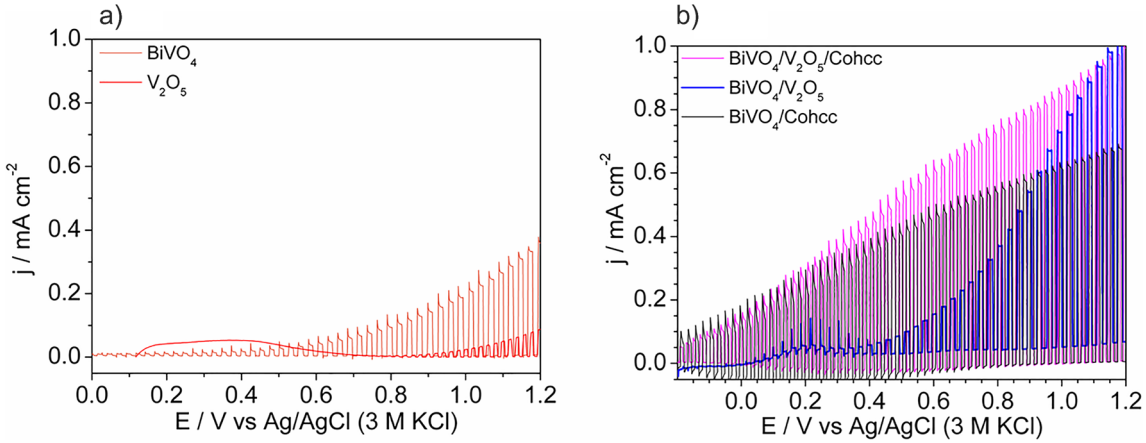

Fig. 4 The linear sweep voltammetry curves of a) FTO/$BiVO_4$ and FTO/V_2O_5, and b) FTO/$BiVO_4$/V_2O_5, FTO/$BiVO_4$/Cohcc (based on previous report [32]) and FTO/$BiVO_4$/V_2O_5/Cohcc recorded under intermittent simulated solar light illumination

confined to the surface or a few crystallographic planes of the studied thin film than to the bulk oxide because current response is recorded at relatively high sweep rates. The effect of cation intercalation/deintercalation in aqueous electrolytes is even more pronounced for K^+ cations [39, 40]. It was reported that electroactivity of V_2O_5 due to the Li^+ intercalation/deintercalation is related to the partial reduction of V^{5+} to V^{4+} centers [41, 42], and it occurs in the aqueous electrolyte as well [43]. The similar effect of dark anodic hump was observed here in the case of $BiVO_4$/V_2O_5 junction; see Fig. 4b. Interestingly, the photocurrent at this range of potential was registered. It is very likely that part of photoexcited holes on $BiVO_4$ took part at V_2O_5 oxidation at a specific range of applied potential (~0–0.4 V), where $BiVO_4$ acts as photoanode ($E > E_{fb}$), but applied potential is lower than E_{fb} of V_2O_5. The LSV curve of FTO/$BiVO_4$/Cohcc photoanode, presented in Fig. 4b for comparison, does not exhibit anodic hump. As it is shown, photoanode without V_2O_5 generates lower photocurrent at a more anodic potential. Lack of heterojunction makes bulk e^-/h^+ recombination easier to occur. However, curves recorded for photoanodes with and without V_2O_5 almost overlapped at a low potential range that is strongly influenced by the presence of cobalt hexacyanocobaltate. Schematically, the effect of V_2O_5 oxidation taking into account band alignment is presented in Fig. 5a. More anodic potential makes V_2O_5 on the electrode already oxidized, and applied potential is higher than flat-band potential of V_2O_5, thus photoexcited holes from both components take part in water photooxidation as it is outlined in a Fig. 5b. There is a significant enhancement of photocurrent generation due to the bulk heterojunction formation and photocurrent reached ~1 mA cm^{-2} at 1.2 V. There are three possible reasons for

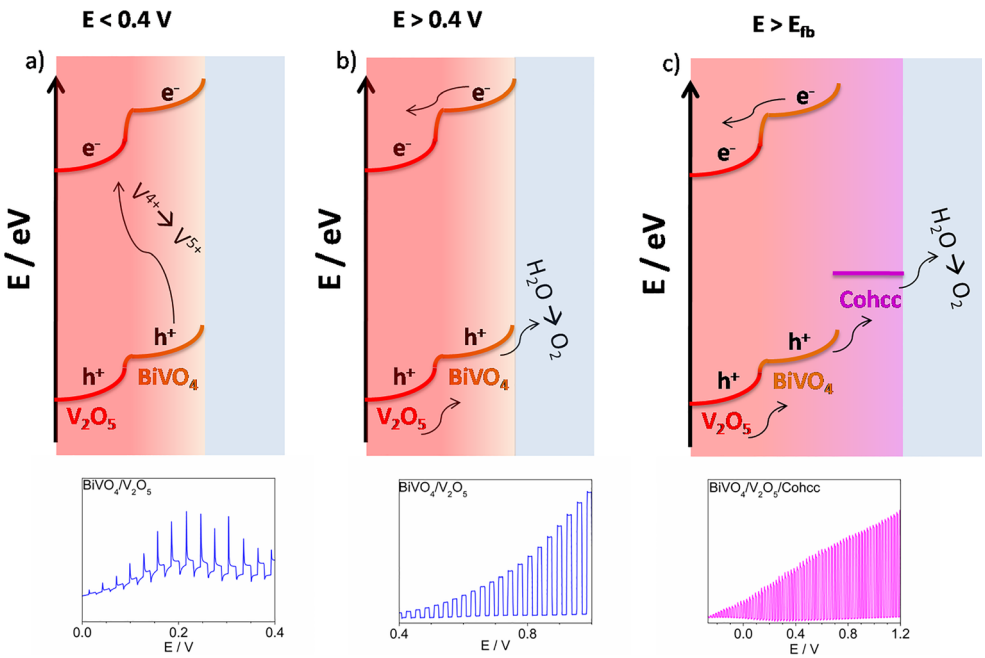

Fig. 5 The schematic presentation of photocurrent generation by a), b) $BiVO_4$/V_2O_5 and c) $BiVO_4$/V_2O_5/Cohcc

increase in photoactivity. The first one is related to the wider range of absorbed radiation due to the narrower energy bandgap of V_2O_5. As it was evidenced (Fig. 4a), photoexcited holes from the V_2O_5 can take part in water photooxidation. The second reason for enhancement is observed due to the heterojunction formation. The internal electric field is generated on the interface between components of photoanode. It significantly enhances e^-/h^+ pairs separation and inhibits bulk recombination. The third one is related to the higher mobility of h^+ of V_2O_5 [33]. $BiVO_4$-based photoanodes required to apply high anodic potential to photooxidize water on its surface efficiently [44]. The common method of onset potential shift towards cathodic direction is based on the $BiVO_4$ modification with oxygen evolution catalysts. Indeed, the presence of Cohcc, which exhibits catalytic properties, makes tested photoanode active in a much wider range of applied potential. Thus, photocurrent of water oxidation is generated at potential more anodic than the flat-band potential of $BiVO_4$ as it is schematically showed in Fig. 5c (effect of V_2O_5 oxidation is probably overlapped). Photocurrent recorded by photoanode with and without Cohcc equalizes over ~1.1 V vs Ag/AgCl (3 M KCl). It is possible to achieve photocurrent on the same range because catalyst (Cohcc) does not affect the absorption ability of investigated photocatalyst. Thus, the formation of $BiVO_4/V_2O_5$ junction increases photocurrent at an anodic range of potential, but surface recombination processes and more anodic location of flat-band potential of V_2O_5 adversely shift onset potential of photocurrent generation in comparison with bare $BiVO_4$. On the other hand, this effect can be eliminated due to the presence of cobalt hexacyanocobaltate on the surface of photoanode.

Conclusions

Four different photoanode arrangements: FTO/$BiVO_4$, FTO/V_2O_5, FTO/$BiVO_4$/V_2O_5, and FTO/$BiVO_4$/V_2O_5/Cohcc were systematically examined using UV-Vis spectroscopy, Raman Spectroscopy, scanning electron microscopy, and electrochemical measurement under intermittent simulated solar light illumination. The phase of V_2O_5 can be formed from the excess of the V-source during the synthesis of $BiVO_4$, and no additional reagents are required. Pulsed laser deposition technique allows obtaining $BiVO_4/V_2O_5$ bulk heterojunction. The photoelectrochemical measurements showed that it is possible to photooxidize V_2O_5 component by photoexcited $BiVO_4$ at some range of applied potential. Applying a higher potential makes $BiVO_4/V_2O_5$ a more efficient photoanode for water oxidation (than bare $BiVO_4$ and V_2O_5) due to the wider utilization of the solar spectrum, improvement of hole mobility, and enhancement of bulk e^-/h^+ separation due to the formation of internal electric field on the $BiVO_4/V_2O_5$ heterojunction. Thus, V_2O_5 improve the photoelectrochemical water splitting, but only at anodic range of applied potential. The $BiVO_4/V_2O_5$/Cohcc photoanode achieved a significantly improved photocurrent density of about 1 mA cm^{-2} at 1.2 V vs Ag/AgCl (3 M KCl) than the individual components: $BiVO_4$ (0.37 mA cm^{-2}) and V_2O_5 (0.90 mA cm^{-2}). However, the enhancement was achieved in a whole range of tested potential, because the presence of Cohcc significantly shifts onset potential of photocurrent generation towards a cathodic direction. In conclusion, a highly efficient $BiVO_4/V_2O_5$/Cohcc heterojunction photoanode was successfully synthesized. The properties of $BiVO_4$-based photoanodes can be tuned *via* proposed modifications. The formation of heterojunction with V_2O_5 significantly affects the values of generated photocurrent, while appropriate cocatalyst (Cohcc) makes possible to photoelectrochemical water splitting at a lower applied potential.

Acknowledgments Author KT gratefully acknowledges financial support from the Statutory Funds of Gdańsk University of Technology (DS 033209). Author M.Sz. is supported by the Foundation for Polish Science.

References

1. S.Y. Tee, K.Y. Win, W.S. Teo, L. Koh, S. Liu, C.P. Teng, Recent progress in energy-driven water splitting. Advanced Science News **4**, 1600337 (2017). https://doi.org/10.1002/advs.201600337
2. A. Fujishima, K. Honda, Electrochemical photolysis of water at a semiconductor electrode. Nature. **238**, 37–38 (1972). https://doi.org/10.1038/239137a0
3. J.K. Cooper, S. Gul, F.M. Toma, L. Chen, S. Liu, J. Guo, J.W. Ager, J. Yano, I.D. Sharp, On the indirect bandgap and optical properties of monoclinic bismuth vanadate. Journal of Physical Chemistry C **119**, 2969–2974 (2015). https://doi.org/10.1021/jp512169w
4. S. Stoughton, M. Showak, Q. Mao, P. Koirala, D.A. Hillsberry, S. Sallis, L.F. Kourkoutis, K. Nguyen, L.F.J. Piper, D.A. Tenne, N.J. Podraza, D.A. Muller, C. Adamo, D.G. Schlom, Adsorption-controlled growth of $BiVO_4$ by molecular-beam epitaxy. APL Materials **1**, 42112 (2013). https://doi.org/10.1063/1.4824041
5. Y. Park, K.J. McDonald, K.S. Choi, Progress in bismuth vanadate photoanodes for use in solar water oxidation. Chemical Society Reviews **42**, 2321–2337 (2013). https://doi.org/10.1039/c2cs35260e
6. K. Tolod, S. Hernández, N. Russo, Recent advances in the BiVO4 photocatalyst for sun-driven water oxidation: top-performing

photoanodes and scale-up challenges. Catalysts **7**, 13 (2017). https://doi.org/10.3390/catal7010013

7. P. Chatchai, Y. Murakami, S. ya Kishioka, A.Y. Nosaka, Y. Nosaka, Efficient photocatalytic activity of water oxidation over WO_3/$BiVO_4$ composite under visible light irradiation. Electrochimica Acta **54**, 1147–1152 (2009). https://doi.org/10.1016/j.electacta.2008.08.058
8. X. Chang, T. Wang, P. Zhang, J. Zhang, A. Li, J. Gong, Enhanced surface reaction kinetics and charge separation of p–n heterojunction Co_3O_4/$BiVO_4$ photoanodes. Journal of the American Chemical Society **137**, 8356–8359 (2015). https://doi.org/10.1021/jacs.5b04186
9. W. Wang, X. Huang, S. Wu, Y. Zhou, L. Wang, H. Shi, Y. Liang, B. Zou, Environmental preparation of p–n junction Cu_2O /$BiVO_4$ heterogeneous nanostructures with enhanced visible-light photocatalytic activity. Applied Catalysis B: Environmental **134–135**, 293–301 (2013). https://doi.org/10.1016/j.apcatb.2013.01.013
10. W.S. dos Santos, L.D. Almeida, A.S. Afonso, M. Rodriguez, J.P. Mesquita, D.S. Monteiro, L.C.A. Oliveira, J.D. Fabris, M.C. Pereira, Photoelectrochemical water oxidation over fibrous and sponge-like $BiVO_4$/β-$Bi_4V_2O_{11}$ photoanodes fabricated by spray pyrolysis. Applied Catalysis B: Environmental **182**, 247–256 (2016). https://doi.org/10.1016/j.apcatb.2015.09.034
11. Z. Tian, P. Zhang, P. Qin, D. Sun, S. Zhang, X. Guo, Novel Black $BiVO_4$/TiO_{2-x} Photoanode with enhanced photon absorption and charge separation for efficient and stable solar water splitting. Advanced Energy Materials **1901287**, 1–8 (2019). https://doi.org/10.1002/aenm.201901287
12. K. Trzciński, M. Szkoda, M. Sawczak, J. Karczewski, A. Lisowska-Oleksiak, Visible light activity of pulsed layer deposited $BiVO_4$/MnO_2 films decorated with gold nanoparticles: the evidence for hydroxyl radicals formation. Applied Surface Science **385**, 199 (2016). https://doi.org/10.1016/j.apsusc.2016.05.115
13. H. Jiang, M. Nagai, K. Kobayashi, Enhanced photocatalytic activity for degradation of methylene blue over V_2O_5/$BiVO_4$ composite. Journal of Alloys and Compounds **479**, 821–827 (2009). https://doi.org/10.1016/j.jallcom.2009.01.051
14. Y. Wang, Y. Long, D. Zhang, Novel bifunctional V_2O_5/$BiVO_4$ nanocomposite materials with enhanced antibacterial activity. Journal of the Taiwan Institute of Chemical Engineers **68**, 387–395 (2016). https://doi.org/10.1016/j.jtice.2016.10.001
15. A.T. Oliveira, M. Rodriguez, T.S. Andrade, H.E.A. De Souza, A.C. Silva, L.L. Nascimento, A.O.T. Patrocínio, High water oxidation performance of W-Doped $BiVO_4$ photoanodes coupled to V_2O_5 rods as a photoabsorber and hole carrier. RRL Solar **1800089**, 1–8 (2018). https://doi.org/10.1002/solr.201800089
16. C.S. Yaw, Q. Ruan, J. Tang, A.K. Soh, M.N. Chong, A Type II n-n staggered orthorhombic V_2O_5/monoclinic clinobisvanite $BiVO_4$ heterojunction photoanode for photoelectrochemical water oxidation: Fabrication, characterisation and experimental validation. Chemical Engineering Journal **364**, 177 (2019). https://doi.org/10.1016/j.cej.2019.01.179
17. X. Xu, S. Kou, X. Guo, X. Li, H. Mao, The enhanced photocatalytic properties for water oxidation over Bi/ $BiVO_4$/V_2O_5 composite. Journal of Physical Chemistry C **121**, 2–10 (2017). https://doi.org/10.1021/acs.jpcc.7b03119
18. M. Arunachalam, K. Ahn, S. Hyung, ScienceDirect Oxygen evolution NiOOH catalyst assisted V_2O_5@$BiVO_4$ inverse opal heterostructure for solar water oxidation. International Journal of Hydrogen Energy **44**, 4656–4663 (2018). https://doi.org/10.1016/j.ijhydene.2019.01.024
19. T.W. Kim, K.-S.K.-S. Choi, Nanoporous $BiVO_4$ photoanodes with dual-layer oxygen evolution catalysts for solar water splitting. Science (80) **343**, 990 (2014). https://doi.org/10.1126/science.1246913
20. Y. Ma, F. Le Formal, A. Kafizas, S.R. Pendlebury, J.R. Durrant, Efficient suppression of back electron/hole recombination in cobalt phosphate surface-modified undoped bismuth vanadate photoanodes. Journal of Materials Chemistry A **3**, 20649–20657 (2015). https://doi.org/10.1039/c5ta05826k
21. S. Wang, P. Chen, J.H. Yun, Y. Hu, L. Wang, An electrochemically treated $BiVO_4$ photoanode for efficient photoelectrochemical water splitting. Angewandte Chemie, International Edition **56**, 8500–8504 (2017). https://doi.org/10.1002/anie.201703491
22. C. Zachäus, F.F. Abdi, L.M. Peter, R. Van De Krol, Photocurrent of $BiVO_4$ is limited by surface recombination, not surface catalysis. Chemical Science **8**, 3712–3719 (2017). https://doi.org/10.1039/c7sc00363c
23. F. Hegner, I. Herraiz-Cardona, D. Cardenas-Morcoso, N. Lopez, J.R. Galan-Mascaros, S. Gimenez, Cobalt hexacyanoferrate on $BiVO_4$ photoanodes for robust water splitting. ACS Applied Materials & Interfaces **9**, 37671 (2017). https://doi.org/10.1021/acsami.7b09449
24. E.P. Alsaç, E. Ülker, S.V.K. Nune, Y. Dede, F. Karadas, Tuning the electronic properties of Prussian blue analogues for efficient water oxidation electrocatalysis: experimental and computational studies. Chemistry - A European Journal **24**, 4856–4863 (2018). https://doi.org/10.1002/chem.201704933
25. M.N. Shaddad, P. Arunachalam, J. Labis, M. Hezam, Fabrication of robust nanostructured (Zr)$BiVO_4$/nickel hexacyanoferrate core/shell photoanodes for solar water splitting. Applied Catalysis B: Environmental **244**, 863–870 (2019). https://doi.org/10.1016/j.apcatb.2018.11.079
26. B. Moss, F.S. Hegner, S. Corby, S. Selim, L. Francas-Forcada, N. Lopez, S. Gimenez, J.R. Galan-Mascarós, J.R. Durrant, Unraveling Charge-transfer in CoFe-Prussian blue modified BiVO 4 photoanodes. ACS Energy Letters **4**, 337 (2019). https://doi.org/10.1021/acsenergylett.8b02225
27. K. Trzciński, M. Szkoda, K. Szulc, M. Sawczak, A. Lisowska-Oleksiak, The bismuth vanadate thin layers modified by cobalt hexacyanocobaltate as visible-light active photoanodes for photoelectrochemical water oxidation. Electrochimica Acta **295**, 410–417 (2019). https://doi.org/10.1016/j.electacta.2018.10.167
28. K. Honma, M. Yoshinaka, K. Hirota, O. Yamaguchi, Fabrication, microstructure and electrical conductivity of V_2O_5 ceramics. Materials Research Bulletin **31**, 531–537 (1996). https://doi.org/10.1016/S0025-5408(96)00015-3
29. S.S. Dunkle, R.J. Helmich, K.S. Suslick, $BiVO_4$ as a Visible-light photocatalyst prepared by ultrasonic spray pyrolysis. Journal of Physical Chemistry C **113**, 11980–11983 (2009). https://doi.org/10.1021/jp903757x
30. M. Hu, N.L. Torad, Y. Yamauchi, Preparation of various Prussian blue analogue hollow nanocubes with Single Crystalline Shells. Eur J Inorg Chem, 4795–4799 (2012). https://doi.org/10.1002/ejic.201200654
31. R.L. Frost, D. Henry, M.L. Weier, W. Martens, Raman spectroscopy of three polymorphs of $BiVO_4$: clinobisvanite, dreyerite and pucherite, with comparisons to $(VO_4)^{3-}$ bearing minerals: namibite, pottsite and schumacherite. Journal of Raman Specroscopy **37**, 722 (2006). https://doi.org/10.1002/jrs.1499
32. C.V. Ramana, O.M. Hussain, B.S. Naidu, P.J. Reddy, Spectroscopic characterization of electron-beam evaporated V_2O_5 thin films. Thin Solid Films **305**, 219–226 (1997). https://doi.org/10.1016/S0040-6090(97)00141-7
33. S.F.A. Kettle, E. Diana, E.M.C. Marchese, E. Boccaleri, P. Luigi, The vibrational spectra of the cyanide ligand revisited : the ν(CN) infrared and Raman spectroscopy of Prussian blue and its analogues. Journal of Raman Specroscopy **2011**, 2006–2014 (2014). https://doi.org/10.1002/jrs.2944
34. J. Roque, E. Reguera, J. Balmaseda, J. Rodríguez-Hernández, L. Reguera, L.F. del Castillo, Porous hexacyanocobaltates(III): Role of

the metal on the framework properties. Microporous and Mesoporous Materials **103**, 57–71 (2007). https://doi.org/10.1016/j.micromeso.2007.01.030

35. B. Zhou, J. Qu, X. Zhao, H. Liu, Fabrication and photoelectrocatalytic properties of nanocrystalline monoclinic $BiVO_4$ thin-film electrode. Journal of Environmental Sciences **23**, 151–159 (2011). https://doi.org/10.1016/S1001-0742(10)60387-7
36. K. Itaya, T. Ataka, S. Toshima, Spectroelectrochemistry and electrochemical preparation method of Prussian blue modified electrodes. Journal of the American Chemical Society **104**, 4767–4772 (1982). https://doi.org/10.1021/ja00382a006
37. J. Su, X.-X. Zou, G.-D. Li, X. Wei, C. Yan, Y.-N. Wang, J. Zhao, L.-J. Zhou, J.-S. Chen, Macroporous $V_2O_5 - BiVO_4$ composites: effect of heterojunction on the behavior of photogenerated charges. Journal of Physical Chemistry C **115**, 8064–8071 (2011). https://doi.org/10.1021/jp200274k
38. M. Yao, P. Wu, S. Cheng, L. Yang, Y. Zhu, M. Wang, H. Luo, B. Wang, D. Ye, M. Liu, Investigation into the energy storage behaviour of layered α-V_2O_5 as a pseudo-capacitive electrode using operando Raman spectroscopy and a quartz crystal microbalance. Physical Chemistry Chemical Physics **19**, 24689–24695 (2017). https://doi.org/10.1039/c7cp04612j
39. Q.T. Qu, Y. Shi, L.L. Li, W.L. Guo, Y.P. Wu, H.P. Zhang, S.Y. Guan, R. Holze, $V_2O_5\ 0.6H_2O$ nanoribbons as cathode material for asymmetric supercapacitor in K_2SO_4 solution. Electrochemistry Communications **11**, 1325–1328 (2009). https://doi.org/10.1016/j.elecom.2009.05.003
40. Q.T. Qu, L.L. Liu, Y.P. Wu, R. Holze, Electrochemical behavior of $V_2O_5\ 0.6H_2O$ nanoribbons in neutral aqueous electrolyte solution. Electrochimica Acta **96**, 8–12 (2013). https://doi.org/10.1016/j.electacta.2013.02.078
41. V. Maurice, S. Zanna, J. Swiatowska-mrowiecka, L. Klein, P. Marcus, XPS study of Li ion intercalation in V_2O_5 thin films prepared by thermal oxidation of vanadium metal. Electrochimica Acta **52**, 5644–5653 (2007). https://doi.org/10.1016/j.electacta.2006.12.050
42. S.D. Perera, A.D. Liyanage, N. Nijem, J.P. Ferraris, Y.J. Chabal, K.J. Balkus, Vanadium oxide nanowire - Graphene binder free nanocomposite paper electrodes for supercapacitors : A facile green approach. Journal of Power Sources **230**, 130–137 (2013). https://doi.org/10.1016/j.jpowsour.2012.11.118
43. N. Cvjetic, I. Pašti, M. Mitric, I. Stojkovic, Electrochemical behaviour of V_2O_5 xerogel in aqueous $LiNO_3$ solution. Electrochemistry Communications **11**, 1512–1514 (2009). https://doi.org/10.1016/j.elecom.2009.05.043
44. Y. Ma, S.R. Pendlebury, A. Reynal, F. Le Formal, J.R. Durrant, Dynamics of photogenerated holes in undoped $BiVO_4$ photoanodes for solar water oxidation. Chemical Science **5**, 2964–2973 (2014). https://doi.org/10.1039/c4sc00469h